

Distribution and growth of thaw slumps in the Richardson Mountains–Peel Plateau region, northwestern Canada



Denis Lacelle^{a,*}, Alex Brooker^a, Robert H. Fraser^b, Steve V. Kokelj^c

^a Department of Geography, University of Ottawa, Ottawa, Ontario, Canada

^b Canada Centre for Mapping and Earth Observation, Ottawa, Ontario, Canada

^c Northwest Territories Geoscience Office, Yellowknife, Northwest Territories, Canada

ARTICLE INFO

Article history:

Received 28 August 2014

Received in revised form 19 January 2015

Accepted 22 January 2015

Available online 2 February 2015

Keywords:

Thaw slumps

Thermokarst

Permafrost

Tasseled Cap transformations

Size-frequency

Northwestern Canada

ABSTRACT

Retrogressive thaw slumps are one of the most active geomorphic features in permafrost terrain. This study investigated the distribution and growth of thaw slumps in the Richardson Mountains and Peel Plateau region, northwestern Canada, using Tasseled Cap (TC) trend analysis of a Landsat image stack. Based on the TC linear trend image, more than 212 thaw slumps were identified in the study area, of which 189 have been active since at least 1985. The surface area of the slumps ranges from 0.4 to 52 ha, with 10 slumps exceeding 20 ha. The thaw slumps in the region are all situated within the maximum westward extent of the Laurentide Ice Sheet. Based on relations between frequency distribution of slumps and that of terrain factors in the landscape, the slumps are more likely to occur on the ice-rich hummocky rolling moraines at elevations of 300–350 m and 450–500 m and along east-facing slopes (slope aspects of 15° to 180°) with gradients of 8° to 12°. Pixel-level trend analysis of the TC greenness transformation in the Landsat stack allowed calculating headwall retreat rates for 19 thaw slumps. The 20-year average retreat rates (1990–2010 period) for 19 slumps ranged from 7.2 to 26.7 m yr⁻¹, with the largest slumps having higher retreat rates. At the regional scale, the 20-yr headwall retreat rates are mainly related to slope aspect, with south- and west-facing slopes exhibiting higher retreat rates, and large slumps appear to be generating feedbacks that allow them to maintain growth rates well above those of smaller slumps. Overall, the findings presented in this study allow highlighting of key sensitive landscapes and ecosystems that may be impacted by the presence and growth of thaw slumps in one of the most rapidly warming region in the Arctic.

Crown Copyright © 2015 Published by Elsevier B.V. All rights reserved.

1. Introduction

Retrogressive thaw slumps are among the most dramatic thermokarst landforms in permafrost terrain (Burn and Lewkowicz, 1990). Thaw slumps typically initiate in regions where ice-rich permafrost is exposed either by: 1) mechanical and thermal erosion caused by fluvial processes and wave action (Lewkowicz, 1987; Couture and Riopel, 2007); 2) thermally driven subsidence along lakeshores (Kokelj et al., 2009); or 3) mass wasting triggered by extreme thaw or precipitation along hillslopes (Aylsworth et al., 2000; Lacelle et al., 2010). The growth of thaw slumps is caused by summer ablation of exposed ice-rich permafrost in headwalls (Lewkowicz, 1987; Grom and Pollard, 2008). Net radiation, summer air temperature, wind and headwall height are the main factors that drive the ablation of ground ice and headwall retreat rates (Lewkowicz, 1985, 1987; Robinson and Pollard, 1998; Grom and Pollard, 2008; Wang et al., 2009). Based on field measurements and analysis of image pairs acquired at decadal to multi-decadal time intervals, headwall retreat rates vary from a few to tens of meters per year

(e.g., Lantuit and Pollard, 2008; Lantz and Kokelj, 2008; Leibman et al., 2008; Lantuit et al., 2012; Swanson, 2012). Thaw slumps will continue to grow as long as the ice-rich permafrost in the headwall remains exposed or until the ground ice supply is exhausted (Burn, 2000). Stabilization often occurs when the rate of slumped debris accumulation at the base of the headwall is greater than the rate of debris removed (French, 1974). Under favorable conditions, thaw slumps may remain active for decades (Burn and Friele, 1989; Kokelj et al., 2013).

The activity of individual thaw slumps has been investigated (Lewkowicz, 1987; Grom and Pollard, 2008), and recent studies have demonstrated the potential impacts of slumps to terrestrial and aquatic environments (Lantuit and Pollard, 2005; Lantz et al., 2009; Lantuit et al., 2012; Kokelj et al., 2013; Malone et al., 2013; Thienpont et al., 2013). However, there are few investigations of the terrain controls on the distribution and growth of thaw slumps at the regional scale, which are required to assess and predict the potential landscape impacts of these permafrost disturbances. In a recent study, Brooker et al. (2014) described a novel approach that can be used to identify the level of activity and monitor the growth of thaw slumps at high temporal resolution. The approach consists of the calculation of the three Tasseled Cap (TC) transformations (brightness, greenness and wetness)

* Corresponding author. Tel.: +1 613 562 5800x1059; fax: +1 613 562 5145.
E-mail address: dlacelle@uottawa.ca (D. Lacelle).

from a dense stack of summer Landsat Thematic Mapper (TM) and Enhanced Thematic Mapper (ETM+) scenes. Given the large footprint and high temporal resolution of Landsat imagery, this method is well-suited for regional scale study of thaw slumps, such as those in north-western Canada (e.g., Aylsworth et al., 2000; Lacelle et al., 2010; Kokelj et al., 2013).

In this study, an inventory of the distribution and growth of thaw slumps in a 15,700 km² area in the Richardson Mountains and Peel Plateau region, Canada, is compiled using data generated with the TC approach. The thaw slumps are classified based on their level of activity (active or stable), and relations between the spatial distribution of thaw slumps and glacial limits, terrain factors (elevation, slope angle, and slope aspect), surface geology and ground ice content in permafrost are explored. Headwall retreat rates for 10% of the active slumps in the region are derived from analyzing variations in the TC greenness transformation at the pixel level in the Landsat stack. The temporal variation in the 3-yr running average retreat rate time-series is compared with climate indices and solar insolation whereas the spatial variation in 20-yr average headwall retreat rates is compared with various terrain factors. Overall, the findings presented in this study allow highlighting sensitive landscapes and terrestrial and freshwater ecosystems that may be impacted by the presence and growth of thaw slumps in one of the most rapidly warming region in the Arctic.

2. Study area

The study area is situated in the Richardson Mountains and Peel Plateau region, northwestern Canada, and includes the following catchments that drain to the Mackenzie Delta or Peel River: Big Fish River, Willow River, Rat River, Stony Creek, Vitrekwa Creek, Road River, Trail River, Caribou River and three small unnamed catchments (Fig. 1). In the Richardson Mountains, elevation is typically more than 500 m, the lowest point being Summit Lake in McDougall Pass (320 m) and the highest point is Mount Sittichinli (1575 m). The Peel Plateau, situated in the southeastern foothills of the Richardson Mountains, consists of a broad, gently eastward-sloping plateau with elevation ranging from 100 to 650 m (Catto, 1996).

The Richardson Mountains separate the unglaciated northern Yukon lowlands to the west from the terrain covered by the Laurentide Ice Sheet during the Late Pleistocene to the east (Duk-Rodkin and Hughes, 1992). The Laurentide Ice Sheet covered the eastern slopes of the Richardson Mountains at ca. 18 ka cal yr BP (Lacelle et al., 2013) up to an approximate elevation of 750 m (Duk-Rodkin and Hughes, 1992). The study area was also affected by two standstills or readvances of the Laurentide Ice Sheet, the Tutsieta Lake Phase dated at ca. 15 ka cal yr BP and an unnamed phase situated a few kilometers east of the Tutsieta Lake Phase (Duk-Rodkin and Hughes, 1992). These two glacial phases are indicated by prominent north-south trending ice-marginal meltwater channels found at an elevation of about 380–420 m. The Richardson Mountains–Peel Plateau region has been ice-free since ca. 13 ka cal yr BP, as suggested by the presence of *Bison priscus* near the community of Tsigetchiic (Zazula et al., 2009). The surface geology in the study area consists mainly of two broad categories. Exposed bedrock and thin colluvial deposits dominate the unglaciated areas in the Richardson Mountains, whereas the glaciated region is covered by till (Hughes et al., 1972; Duk-Rodkin and Hughes, 1992). Hummocky rolling moraines up to 50 m thick occupy the area constrained between the maximum glacial limit and the Tutsieta Lake Phase limit, whereas broad morainal plains less than 20 m thick is found in the area east of the Tutsieta Lake Phase (Hughes et al., 1972; Duk-Rodkin and Hughes, 1992). A series of post-glacially incised river and stream valleys dissect the Richardson Mountains and Peel Plateau with several reaches of the modern rivers and streams occupying sections of the paleo-meltwater channels. The fluvial incision has resulted in a dendritic network characterized by V-shaped valleys in the uplands with relief between the thalwegs being less than few meters that evolve

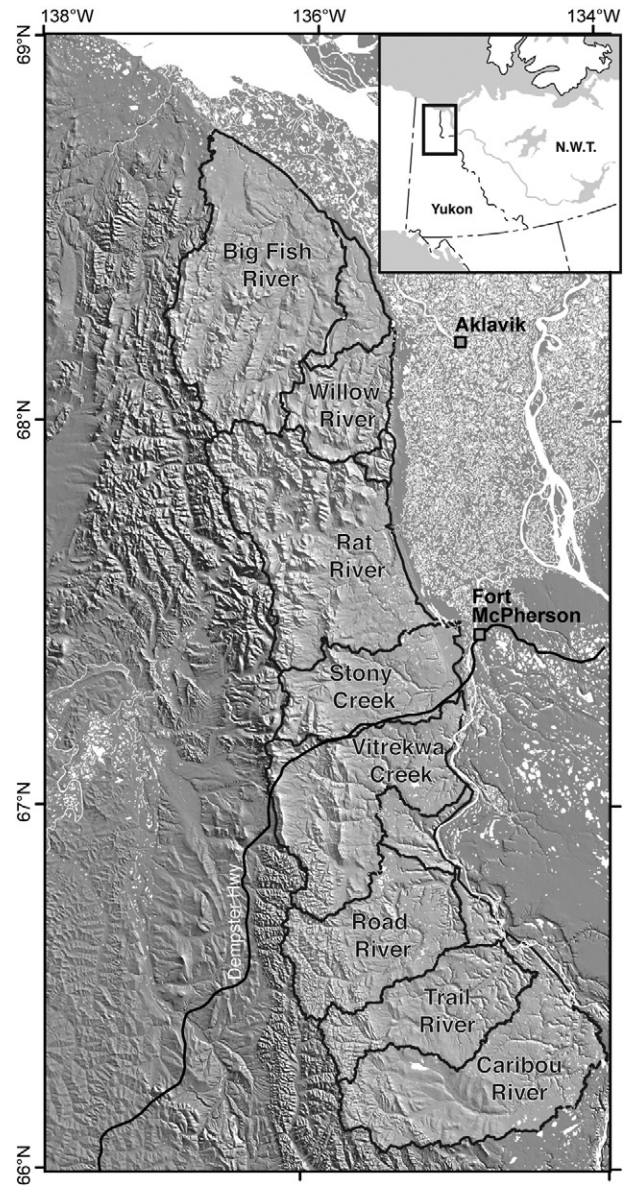


Fig. 1. Map showing the location of the study area (Big Fish River to Caribou River sub-basins) in the Richardson Mountains–Peel Plateau region, northwestern Canada. Hillshade background image derived from 30 m Canadian Digital Elevation Data (www.geogratis.ca).

to canyon-type valleys with relief of ca. 350 m near the confluence with the Mackenzie and Peel rivers.

The climate in the region is characterized by long cold winters and short cool summers. The mean annual air temperature in Fort McPherson (1986–2010), the closest meteorological station, is -6.8 ± 1.6 °C (Environment Canada, 2012). July is the warmest month with average temperatures of 15 °C, whereas the coldest temperatures occur in January with an average of -27 °C. Since the 1970s, mean annual air temperatures have increased at a rate of 0.77 °C per decade in western Arctic Canada (Burn and Kokelj, 2009), making this one of the most rapidly warming regions on the planet (Serreze et al., 2000). However, for the period covered by Landsat imagery (1986–2012), the mean annual air temperature in Fort McPherson shows a non-significant warming trend (0.034 °C yr⁻¹; $p = 0.31$), whereas the mean summer air temperature shows a non-significant cooling trend (-0.036 °C yr⁻¹; $p = 0.29$). Total annual precipitation in Fort McPherson (1986–2007) averages 295 mm, with rainfall accounting for approximately half (148 mm) (Environment Canada, 2012). Rainfall in the area occurs mainly from convective

Table 1
Landsat satellite scenes used for the calculation of the three Tasseled Cap transformations and creating the image stacks for the Tasseled Cap linear trend image.

Path-row	Year	Month	Day	Sensor type
<i>North stack</i>				
64-12	1985	8	5	L5
64-12	1986	8	8	L5
64-12	1989	7	15	L5
64-12	1991	7	5	L5
63-12	1992	8	1	L5
63-12	1993	8	20	L5
63-12	1994	8	7	L5
63-12	1996	7	11	L5
63-12	1997	7	30	L5
64-12	1999	8	4	L7
63-12	2001	7	17	L7
64-12	2004	8	9	L7
63-12	2007	7	10	L7
64-12	2009	8	23	L7
63-12	2010	7	10	L7
64-12	2011	7	28	L7
<i>South stack</i>				
63-13	1988	7	5	L5
62-13	1990	7	4	L5
63-13	1991	6	28	L5
62-13	1992	7	9	L5
62-13	1993	7	28	L5
63-13	1994	8	7	L5
62-13	1995	7	2	L5
63-13	1998	7	1	L5
62-13	2000	7	7	L7
63-13	2004	7	1	L7
62-13	2004	7	2	L7
62-13	2004	7	26	L7
62-13	2005	6	27	L7
62-13	2006	8	1	L7
62-13	2007	8	12	L7
62-13	2009	7	16	L7
62-13	2010	8	4	L7
62-13	2011	6	28	L7

storms. Since 1986, a significant rising trend in total June–July rainfall is observed (0.31 mm yr^{-1} ; $p < 0.05$). Vegetation consists of open spruce woodlands in the valley bottoms and south-facing slopes (*Picea* spp., *Populus balsamifera*) transitioning to dwarf shrub (*Betula* spp., *Alnus* spp., *Salix* spp.) and sub-Arctic tundra (*Cyperaceae* spp., *Eriophorum angustifolium*) on the plateau (Ecosystem Classification Group, 2010).

These climate and vegetation conditions ensure that permafrost is continuous in the Richardson Mountains and Peel Plateau region (Heginbottom and Radburn, 1992). The ground ice content in the

study area has not been well characterized and is likely highly variable. The Permafrost Map of Canada (Heginbottom and Radburn, 1992) indicates that ground ice content in the study area is generally less than 20 vol.%. However, measurements from the headwall of six thaw slumps in the Willow River and Stony Creek sub-basins indicate that the ground ice content in the uppermost 10 m of permafrost ranges from 50 vol.% to tabular bodies of massive ground ice (Lacelle et al., 2004, 2010; Malone et al., 2013). In addition, qualitative data from seismic shothole record indicate the presence of layers of massive ice of known thickness within the uppermost 2 m of permafrost in 50% of the 131 shotholes in the study area (Smith and Lesk-Winfield, 2012).

3. Methodologies

3.1. Tasseled Cap trend analysis and identification of thaw slumps

The Landsat TC trend analysis approach used in this study follows the methodology described by Fraser et al. (2011, 2012) and Brooker et al. (2014). To create the Landsat image stack, 35 level-1 terrain corrected Landsat TM and ETM+ summer scenes (late June to late August) with minimal cloud cover (<10%) between the years of 1985 and 2011 were acquired from the United States Geological Survey Glovis website (<http://glovis.usgs.gov>). However, due to significant cloud cover during some years, Landsat images were not acquired each year (Table 1). The Landsat scenes were combined into a single .pix file in PCI Geomatica 10 software and each channel was calibrated to top-of-atmosphere reflectance using USGS coefficients (Chander et al., 2009) and screened for cloud, cloud shadow and missing scan line data (Zhu and Woodcock, 2012). The three TC transformations, brightness, greenness and wetness were then calculated for each image (Table 2 in Brooker et al. (2014)) and combined into a single image stack so that linear trends for each transformation could be computed using robust Theil–Sen regression (Fraser et al., 2012). Integer versions of the TC trend (slope) images were then derived for easier visualization by applying a scaling factor of 1000. The three TC index trends were combined into a single RGB image (i.e. brightness slope = red, greenness slope = green, and wetness slope = blue) to generate a color image representing the three-dimensional TC trajectory, the linear trend TC image (Fraser et al., 2014).

3.2. Distribution of thaw slumps and controls on their occurrence

The distribution of active and stable thaw slumps in the Richardson Mountains–Peel Plateau region was mapped using the linear trend TC image (Fig. 2). Each thaw slump was traced in ArcGIS 10 software and

Table 2

Location, terrain characteristics of the 19 randomly selected thaw slumps in the Richardson Mountains–Peel Plateau region. Column “code” refers to labels in Fig. 7.

Name	Code	Watershed	Latitude	Longitude	Area (ha)	Elevation (m)	Aspect	20-yr retreat rate (m yr^{-1})
Slump 1	1	Rat	67.588	–135.798	8	390	88	12.8
Slump 2	2	Rat	67.586	–135.751	9	320	307	7.3
Slump 3	3	Rat	67.520	–135.303	11	236	48	7.2
Slump 9	4	Stony Creek	67.341	–135.330	7	204	345	11.3
FM4	5	Stony Creek	67.277	–135.160	20	259	38	9.4
FM2 (Charas)	6	Stony Creek	67.255	–135.234	48	318	323	15.0
Slump 10	7	Stony Creek	67.252	–135.759	5	531	104	9.4
FM3 (Melanie)	8	Stony Creek	67.252	–135.268	10	382	33	12.5
Slump 2	9	Stony Creek	67.241	–135.823	14	643	53	15.0
Dover	10	Vittrekwa	67.116	–135.800	21	619	69	26.7
Slump 11	11	Vittrekwa	67.103	–135.690	5	459	141	13.1
Slump 6	12	Vittrekwa	67.065	–135.760	8	518	27	11.3
Tiny slump	13	Vittrekwa	66.974	–135.526	11	305	221	19.0
Medium slump	14	Vittrekwa	66.938	–135.540	18	363	169	13.8
Slump 13	15	Road	66.670	–134.916	9	353	299	13.8
Slump 12	16	Road	66.613	–135.157	9	370	342	10.0
Slump 15	17	Trail	66.549	–135.174	5	340	105	7.6
Small slump	18	Trail	66.468	–135.402	7	452	104	9.0
Slump 16	19	Trail	66.429	–135.147	12	483	37	11.7

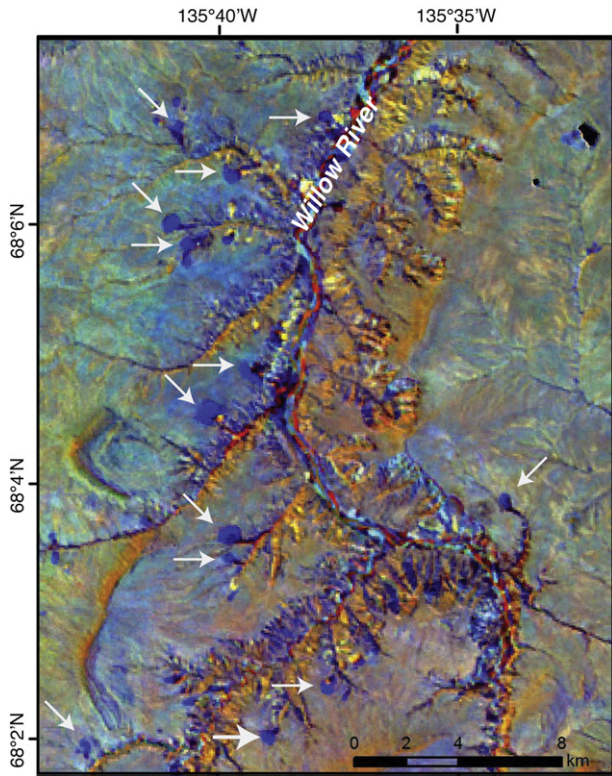


Fig. 2. Tasseled Cap linear trend image used to identify the distribution of thaw slumps. Image is showing a portion of the Willow River catchment (arrows are pointing to thaw slumps). Blue colors (representing increasing TC wetness) are associated with the wet and active portion of the slump floor; red colors (representing increasing TC brightness) are associated with dry and un-vegetated surfaces of the slump floor. The teal and yellow colors (representing increasing TC greenness) correspond to portion of the slump floor that is stable and undergoing regrowth by colonizing vegetation.

the centroid of each polygon determined. The planimetric area of each slump was obtained by calculating the surface area of each polygon in ArcGIS. To investigate controls of terrain attributes, surface geology, ground ice content and glacial limits on the distribution of thaw slumps, the slump inventory was placed over a 30 m resolution digital elevation model (DEM; data from the Canadian Digital Elevation Data, www.geogratis.ca). Terrain attributes, which include elevation, slope angle, slope aspect and slope curvature, were derived using ArcGIS Spatial Analyst. Since the DEM was created from ca. 1950s topographic maps, these attributes represent slope conditions prior to the initiation of most thaw slumps. The glacial limits (maximum extent of the Laurentide Ice Sheet, Tutsieta Lake Phase) were digitized from the maps of Hughes et al. (1972) and Duk-Rodkin and Hughes (1992). The surface geology is derived from the geospatial dataset of Cote et al. (2013). Measurements on ground ice content in the study area are limited to six slumps (Lacelle et al., 2010, 2013) and 131 qualitative seismic shothole logs (Smith and Lesk-Winfield, 2012). The occurrence of massive ice layers of known thicknesses within the uppermost 2 m of permafrost was assessed from the seismic shothole logs and compared to the surface geology and location of thaw slumps. To determine whether the frequency distribution of thaw slumps reflects the frequency distribution of terrain factors in the landscape, or if some components are associated with an enhanced probability of thaw slump occurrence, the thaw slump frequency was normalized by the frequency distribution of terrain factors.

It should be noted that active and stable thaw slumps identified from the TC linear trend image might not capture every thaw slump in the study area. The identification of thaw slumps is limited by the pixel

resolution of the Landsat images (30 m) and features <0.36 ha are likely not mapped. In addition, Dyke (2004) documented the presence of both thaw slumps and rotational slope failures on the Peel Plateau. Since the linear trend TC image cannot distinguish between the various types of landslides (i.e., rotational or translational slope failures and thaw slumps), it is possible that some of the features in this region do not represent thaw slumps *sensu stricto*.

3.3. Calculation and analysis of controls on headwall retreat rates

The 35 level-1 terrain corrected Landsat TM and ETM+ summer scenes have sub-pixel multi-temporal registration accuracy, which allows for headwall retreat rates to be calculated from the Landsat stack (Brooker et al., 2014). For 19 randomly selected active thaw slumps in the study area (Table 2), the greenness transformation pixel values for each Landsat scene in the stack was extracted along a linear transect of 10 to 15 adjoining pixels using the Sample function in ArcGIS Spatial

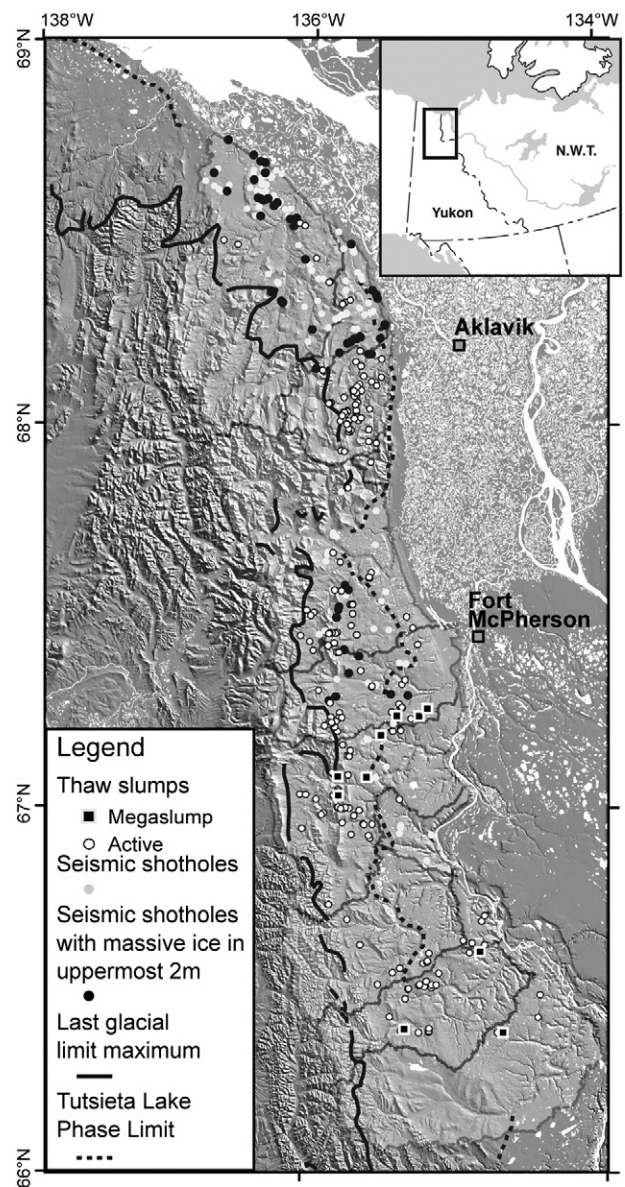


Fig. 3. Map showing the distribution of active and stable thaw slumps, including mega-slumps in the Richardson Mountains–Peel Plateau region, northwestern Canada, using the Tasseled Cap trend analysis of dense Landsat image stack. Hillshade background image derived from 30 m Canadian Digital Elevation Data (www.geogratis.ca); seismic shotholes data derived from Smith and Lesk-Winfield (2012).

Analyst. For each slump, the transect started from the slump floor, intersected the apex of the arcuate-shaped headwall, and extended 1 to 2 pixels upslope of the position of the headwall on the 2011 Landsat scene. The single-date greenness transformation values were plotted against the year of the Landsat scene to generate a time-series of greenness changes for each pixel along the transect. In the study area, the greenness values for undisturbed open spruce surfaces are >100 and decrease to <50 as the headwall retreats across the pixel and the surface changes to a muddy slump floor (Brooker et al., 2014). As such, headwall retreat rates were calculated by determining the years at which the greenness time-series for each pixel intersected the threshold value of 50 using the following equation (Brooker et al., 2014):

$$HR_{(x_i-x)} = \frac{PR}{T_{x_i} - T_x} \quad (1)$$

where: $HR_{(x_i-x)}$ = retreat rate for the period between years x_i and x (in m yr^{-1}); PR = pixel resolution (in m; 30 m for linear transect and 42 m for diagonal transect); T = year of intersection of the greenness time-series for pixels x_i and x with the threshold value of 50.

The headwall retreat rate calculated using Eq. (1) provides values averaged over the time period required for the headwall to retreat 30 m. Considering that the Landsat stack is missing some years (Table 1), the 1-yr average retreat rates might not accurately reflect headwall retreat rates at this time-scale. As such, we present the headwall retreat rates as 3-yr running average and 20-yr average. For the latter, Brooker et al. (2014) showed that the calculated retreat rates are similar to those obtained from high-resolution satellite images.

The temporal variation of the 3-yr running average headwall retreat rates of the 19 slumps was compared to mean summer air temperature, thaw degree-days (data from Fort McPherson meteorological station; Environment Canada, 2012) and total solar irradiance (data from the Lasp Interactive Solar Irradiance Datacenter; <http://lasp.colorado.edu/lisird>). Relations between the 3-yr running average headwall retreat rates and temperature and total solar irradiance were investigated using linear regressions.

The spatial variation of the 20-year average headwall retreat rates of the 19 active thaw slumps was assessed by performing linear regression analyses between the 20-yr retreat rates and: i) terrain factors (elevation, aspect, slope angle, and slope curvature) and potential incoming solar radiation ($PISR$); ii) surface area of the slump; and iii) potential effect of surface and active layer runoff. $PISR$, expressed in W m^{-2} , was derived using the Solar Analyst module in ArcGIS. Since the thaw slumps grow during the summer (June–August), the solar radiation reaching the surface was calculated for each summer using a mean cloud cover factor of 30% and averaged for the 1990–2010 period. The potential effect of surface and active layer runoff on 20-yr average headwall retreat rates was investigated by calculating two topographic indices representing relative moisture contribution. The first, flow accumulation, represents the upslope area draining into each cell on the landscape and provides a measure of the quantity of water delivered. The second, a topographic moisture index, is derived by dividing flow accumulation by the local slope angle representing hydraulic gradient (Beven and Kirkby, 1979). Soil saturated areas are predicted to occur at sites where this index exceeds a specified threshold.

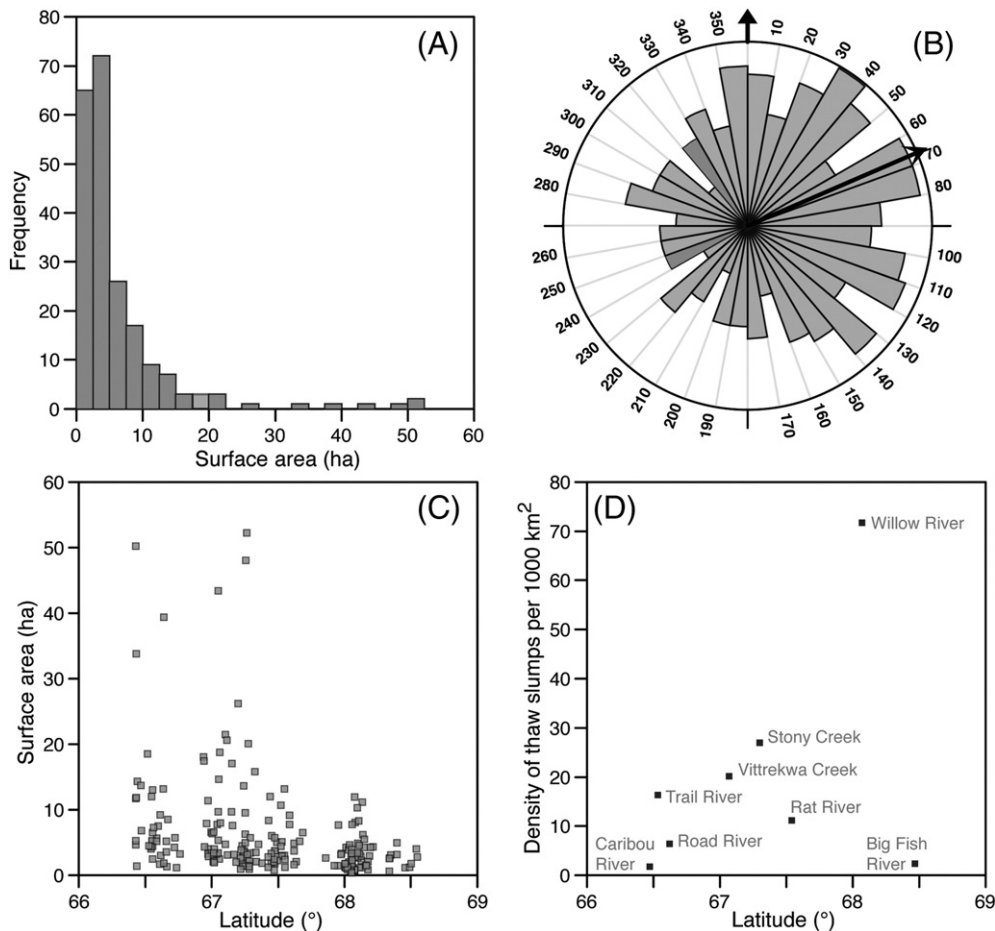


Fig. 4. Frequency distribution of surface area of thaw slumps (A), orientation of thaw slumps (B), surface area latitude of thaw slumps (C), and density of thaw slumps (D) in the Richardson Mountains and Peel Plateau, northwestern Canada. See Fig. 1 for delineation of the catchments named in (D).

4. Results

4.1. Distribution of thaw slumps and controls on their occurrence

In the Richardson Mountains–Peel Plateau region, 212 thaw slumps were identified based on the linear trend TC image, 189 of which are classified as being active (Fig. 3). The surface area of mapped thaw slumps ranges from 0.4 ha (the minimal size of feature identifiable using Landsat imagery) to 52 ha, with an average of 5.4 ha (Fig. 4A).

The largest slumps in the mapping region are greater than 20 ha and are termed mega-slumps. Out of the 212 slumps identified, 10 mega-slumps are identified, all of which are situated within the southern region (Fig. 4C). These mega-slumps are all active and the sum of their surface area accounts for 27% of all mapped active slumps. The density of thaw slumps shows a latitudinal distribution (Fig. 4D). The density of thaw slumps is generally higher in the northern region, with the Willow River, Stony Creek and Vittrekwa River catchments containing the highest density of slumps. Together, these three watersheds account

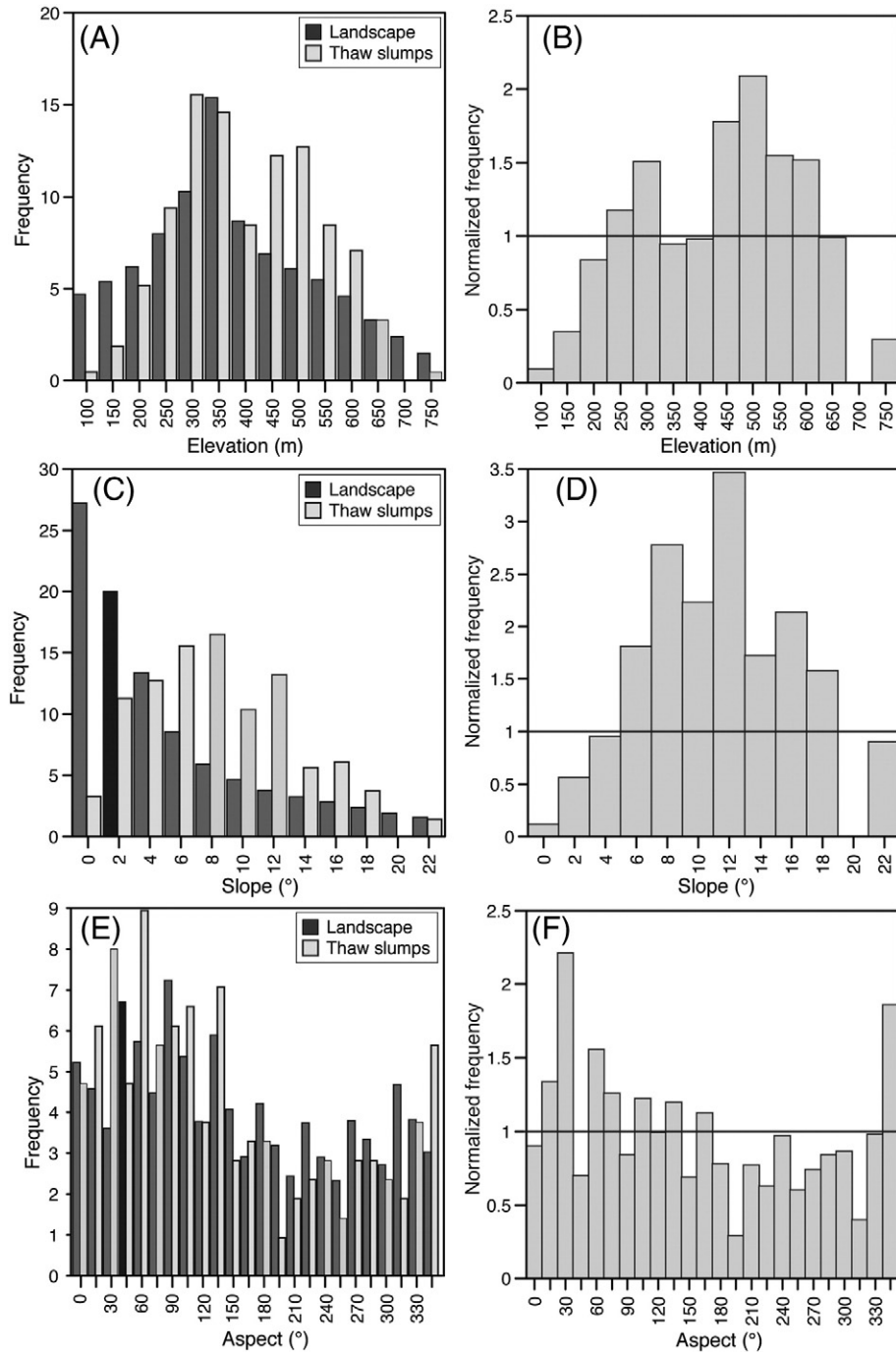


Fig. 5. Frequency distribution of thaw slumps and terrain factors in the Richardson Mountains–Peel Plateau region, northwestern Canada. A) Histogram showing the fraction of thaw slumps mapped in each elevation class (50 m bins) and the fraction of the study area DEM falling within each elevation class. B) Enhancement factor of elevation on occurrence of thaw slumps in the landscape. Values greater than 1 indicate that thaw slumps occur preferentially at these elevations. C) Histogram showing the fraction of thaw slumps mapped in each slope class (2° bins) and the fraction of the study area DEM falling within each slope class. D) Enhancement factor of slope on occurrence of occurrence of thaw slumps in the landscape. Values greater than 1 indicate that thaw slumps occur preferentially at these slopes. E) Histogram showing the fraction of thaw slumps mapped in each aspect class (15° bins) and the fraction of the study area DEM falling within each aspect class. F) Enhancement factor of aspect on occurrence of thaw slumps in the landscape. Values greater than 1 indicate that thaw slumps occur preferentially at these slope aspects.

for nearly 60% of all slumps identified, but comprise only 25% of the total study area.

In the study area, all thaw slumps are situated within the maximum westward extent of the Laurentide Ice Sheet, with 69% of the slumps being constrained between the maximum glacial extent and the Tutsieta Lake Phase limit (i.e., on the hummocky rolling moraines) (Fig. 3). The hummocky moraines occupy 46% of the study area, whereas the broad morainal plains occupy 31%. Normalizing the distribution of slumps by the area occupied surface deposits indicate that slumps are more likely to occur on the hummocky rolling moraines by a factor of 1.5. The relations between the distribution of thaw slumps with terrain factors (elevation, slope angle, and aspect) was explored by comparing the frequency distribution of thaw slump with each variable within the glaciated portion of the study area (Fig. 5). Thaw slumps in the study area are observed at elevation ranging from 112 to 765 m. To explore relations with elevations, the slump and landscape elevations

were grouped into 50 m bin classes. Elevation in the landscape shows a normal distribution, whereas the thaw slumps have a bi-modal distribution (dominant modes found at 300–350 m and 450–500 m). The normalized distribution of thaw slumps by the frequency distribution of elevation in the landscape indicates that slumps are more likely to occur at elevations of 450–600 m by a factor of 2 and by a factor of 1.5 at elevations of 250–300 m (Fig. 5B). To explore relations with hillslope gradients, the slump and landscape slope angles were binned into 2° classes. The hillslope gradients in the landscape show an exponential decrease in frequency. The thaw slumps are all found on slope angles <23° and their frequency shows a near normal distribution with 43% of slumps found on hillslopes of 4–8°. However, normalizing the distribution of thaw slumps by the frequency distribution of hillslope gradients in the landscape reveals that slump are more likely to occur by a factor of 2 to 3 on slopes of 8 to 12° (Fig. 5D). The study area is situated along the eastern flank of the Richardson Mountains and Peel Plateau and combined with the development of the fluvial network, east-facing slopes are predominant on this landscape. Even though thaw slumps in the study area are found on slopes of all aspects, they are predominantly observed on east facing slopes (vector mean of 69°). Normalizing the frequency distribution of thaw slumps by the frequency of slope aspects in the landscape reveals that slumps are more likely to occur on North to North-East slopes (330° to 30°) by a factor of 2, while normalized frequency >1 is observed on North East to South East slopes (slope aspects of 15° to 180°; Fig. 5F).

4.2. Headwall retreat rates of thaw slumps

The headwall retreat rates for 19 randomly selected thaw slumps in the Richardson Mountains–Peel Plateau region were calculated using Eq. (1). The 1-yr average headwall retreat rates for the 19 slumps ranged from 5 to 60 m yr⁻¹, with an average of 12.4 ± 7.4 m yr⁻¹. Fig. 6 shows the 3-yr running average between 1990 and 2010 along with the 3-yr running average mean summer air temperature, thaw degree-days and total solar irradiance. The 3-yr running average retreat rates show high temporal variability, with maximum retreat rates observed in the mid-1990s and mid-2000s. Correlation analysis indicates that only a few slumps have statistically significant (10% level) correlation between their 3-yr running average headwall retreat rates and mean summer air temperature, thaw degree-days and total solar irradiance (Table 3).

The 20-year average headwall retreat rates of the 19 slumps ranged from 7.2 to 26.7 m yr⁻¹, with the two mega-slumps ranking in the top

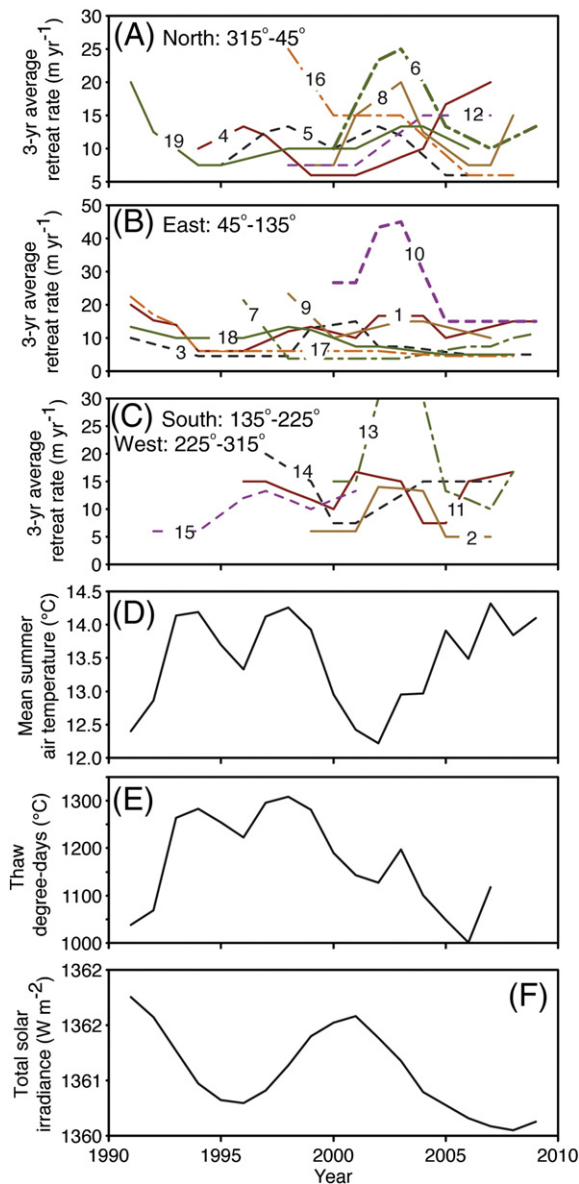


Fig. 6. 3-yr running average headwall retreat rates for 19 randomly selected thaw slumps in the Richardson Mountains–Peel Plateau region, northwestern Canada: (A) North-facing slumps, (B) East-facing slumps, (C) South- and West-facing slumps. Also shown are the 3-yr running average mean summer air temperature (D), thaw degree-days (E), and total solar irradiance (F). Headwall retreat rates were calculated using Eq. (1). Location, terrain characteristics and 20-yr average headwall retreat rates of the 19 thaw slumps are provided in Table 2.

Table 3

Correlation coefficient (*r*) between 3-yr running average of headwall retreat rates and mean summer air temperature (MSAT), Thaw degree-days (TDD) and total solar irradiance (TSI) for 19 active thaw slumps in the study area. Correlations significant at the 10% level are indicated in bold.

Name	Watershed	3-yr MAST	3-yr TDD	3-yr TSI
Slump 1	Rat	-0.42	-0.46	0.34
Slump 2	Rat	-0.61	0.16	0.19
Slump 3	Rat	-0.57	-0.12	0.77
Slump 9	Stony Creek	0.49	-0.49	-0.91
FM4	Stony Creek	-0.26	0.50	0.65
FM2 (Charas)	Stony Creek	-0.67	0.36	0.43
Slump 10	Stony Creek	0.29	0.15	-0.57
FM3 (Melanie)	Stony Creek	-0.60	0.13	0.21
Slump 2	Stony Creek	0.35	0.66	0.10
Dover	Vittrekwa	-0.81	0.66	0.69
Slump 11	Vittrekwa	-0.07	0.17	-0.07
Slump 6	Vittrekwa	0.21	-0.76	-0.89
Tiny slump	Vittrekwa	-0.62	0.40	0.33
Medium slump	Vittrekwa	0.81	0.28	-0.68
Slump 13	Road	-0.09	0.91	0.73
Slump 12	Road	-0.25	0.12	-0.06
Slump 15	Trail	0.03	0.53	0.59
Small slump	Trail	-0.34	-0.25	0.64
Slump 16	Trail	-0.57	-0.60	0.51

three highest values (Table 2). If we remove the two mega-slumps, the maximum 20-yr retreat rates decrease to 19 m yr^{-1} . Considering that the 20-yr headwall retreat rates represent the average value for each of the 19 slumps, we explored possible terrain factors that could explain the spatial variability in the 20-yr headwall rates. The 20-yr retreat rates of each slump, including the two mega-slumps, was regressed against

their respective elevation, slope angle, transformed aspect, PISR, topographic moisture index, flow accumulation and surface area (Fig. 7). The single factor correlation analysis reveals statistically significant relations (10% level) with transformed aspect ($r^2 = 0.33$), PISR ($r^2 = 0.11$) and elevation ($r^2 = 0.19$) and with surface area showing a near-statistically significant relation ($r^2 = 0.14$; $p = 0.12$); no relation was

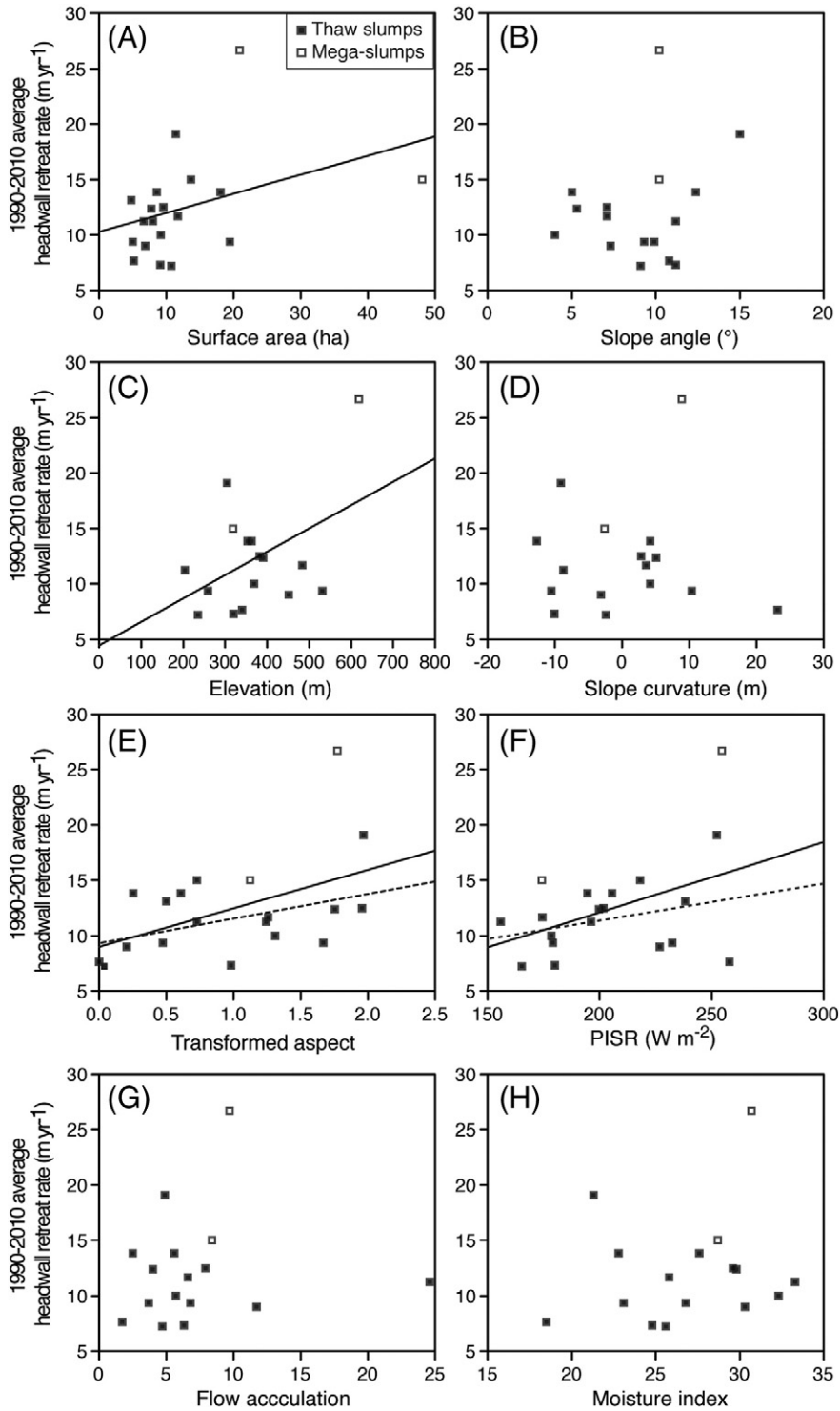


Fig. 7. Scatterplots of 20-yr average headwall retreat rates and various terrain factors. A) Surface area. B) Slope angle. C) Elevation. D) Slope curvature. E) Transformed aspect. F) Potential incoming solar radiation. G) Flow accumulation. H) Moisture index. The slope aspect variable (expressed as slope degree) was transformed to a linear variable where north-east slopes = 0 (least exposed to the sun) and south-west facing slopes = 2 following the model of Beers et al. (1966): transformed aspect (A') = $\cos(45^\circ - \text{aspect}) + 1$. The slope curvature (or shape) was computed from the second derivative of the fourth-order polynomial surface fitted to a local 3-by-3 window using the Grid's Curvature function in ArcGIS 10 software. A positive value means the surface is convex (situated near shoulder of the hillslope) while a negative value indicates the surface is concave (situated near the footslope). Linear regression lines are shown for statistically significant to near-significant relations (solid line includes the mega-slumps; dashed line excludes the mega-slumps). Coefficients of linear regression are shown in Table 3.

found with other factors (Table 4). If we exclude the two mega-slumps from the regression analysis, only transformed aspect ($r^2 = 0.30$) has a statistically significant relation; all other terrain factors have no relation with 20-yr average retreat rates (Table 4).

5. Discussion

5.1. Relation between the distribution of thaw slumps and landscape factors

The distribution of thaw slumps in a landscape is related to the mechanism(s) that exposes ice-rich permafrost, which may lead to the initiation of thaw slumps. This study revealed that thaw slumps in the Richardson Mountains–Peel Plateau region are more likely to occur on the hummocky rolling moraines at elevations of 300–350 m and 450–500 m and along east-facing slopes (slope aspects of 15° to 180°) with gradients of 8° to 12° (Fig. 5).

The hummocky rolling moraines are particularly sensitive to contain thaw slumps as the till veneer is ice-rich and fluvial incision has provided relative relief that promotes slope instability and downslope removal of slumped materials. In fact, 48% of the 94 shotholes in the hummocky moraines contain layers of massive ice within the uppermost 2 m of permafrost (Fig. 3). Conversely, the broad morainal plain that is situated east of the Tutsieta Lake Phase limit contains 31% of the thaw slumps, and only 19% of the 37 shotholes in the morainal plain contains massive ice within the uppermost 2 m of permafrost. Based on these relations, it appears that the near-surface permafrost in the hummocky moraines constrained between the maximum westward extension of the Laurentide Ice Sheet and the Tutsieta Lake Phase limit is ice-rich and prone to host thaw slumps. One exception in this zone would be the paleo-meltwater channels where no thaw slumps are found. In the area east of the Tutsieta Lake Phase limit, the landscape contains fewer thaw slumps but kettle lakes are abundant. Considering that the presence of kettle lakes tends to be associated with ice-cored terrain (Benn and Evans, 2010), as observed in central Yukon (Beirle, 2002; Lacelle et al., 2007) and Bylot Island (Moorman and Michel, 2000), it is likely that the area between the Tutsieta Lake phase limit and the Peel River is ice-cored. Such a landscape typically results in a patchy distribution of bodies of massive ground ice in the permafrost and thaw slumps would only form if an initiation mechanism exposes these ice bodies, otherwise a slump may not develop.

In the study area, the initiation of hillslope thaw slumps is mainly related to the stream network development and fluvial processes (Kokelj et al., in review). Field observations revealed that many thaw slumps initiated either at different position on the hillslope along water-tracks, the latter forming following periods of heavy rainfall and mass wasting, or at the base of the hillslope following stream undercutting of the slope (Fig. 8). The fact that thaw slumps are more likely to occur on moderately steep slopes (8° to 12°) would facilitate the mass wasting of material following heavy rainfall periods, help to move the thawed material downslope, and maintain the ice-rich permafrost exposed.

The observation that hillslope thaw slumps in the Richardson Mountains–Peel Plateau are predominantly found on east facing slopes



Fig. 8. Field photograph (late July 2011) showing the initiation of a thaw slump along a water-track on a hillslope in the Stony Creek watershed.

(slope aspects of 15° to 180° ; Fig. 5F) is inconsistent with the orientation of thaw slumps along shorelines of lakes in the nearby Mackenzie Delta, where slumps are mainly found along south and west facing shorelines (Kokelj et al., 2009). The preference for hillslope thaw slumps to initiate on east facing slopes might be a topographic effect. In mountainous regions, such as in the Richardson Mountains–Peel Plateau, the active layer may be thicker along south and west facing slopes due to the higher amount of insolation received along these slopes. In ice-rich permafrost environment, the difference in active layer thickness due to slope orientation typically leads to the development of asymmetric valleys, with shallower south and west facing slopes caused by the melting of near-surface ground ice and associated subsidence of the surface (i.e., French, 2007). Fig. 9 shows topographic cross-sections for nine fluvial valleys in the Stony Creek and Vittrekwa catchments. For most cross-sections, a valley asymmetry is observed with steeper north and east facing slopes. Therefore, because valley asymmetry is observed along the hillslopes, the predominance of thaw slumps to develop along east facing slopes is likely due to the ice-rich permafrost being found closer to the ground surface along these slopes (i.e., shallower active layer). This would facilitate a triggering mechanism of thaw slumps, such as mass wasting triggered by extreme thaw or precipitation along water tracks, to expose the near-surface ice-rich permafrost. In the adjacent Mackenzie Delta region, this topographic control of varying active layer thickness does not occur due to flat terrain; hence the predominance of modern lakeshore thaw slumps to be exposed along the warmer south and west lakeshores (Kokelj et al., 2009).

Overall, it appears that the ice-rich permafrost conditions required for the initiation and growth of thaw slumps in the Richardson Mountains–Peel Plateau region are largely a heritage of the last glaciation. The thaw slumps are mostly constrained to glacial tills and morainal deposits proximal to major ice-front positions, including the maximum extent of the Laurentide Ice Sheet and the Tutsieta Lake Phase. The distribution of modern thaw slumps reflects general landscape morphology associated with east facing regional slope and the ongoing fluvial processes and stream network development that have produced moderately steep hillslopes.

5.2. Relation between headwall retreat rates and landscape factors

Our analysis of 19 thaw slumps in the Richardson Mountains–Peel Plateau region revealed that only a few slumps had a significant high degree of correlation between their 3-yr running average headwall retreat rates and summer air temperatures or total solar irradiance (Fig. 6; Table 3). This is in contrast to the result of past studies: at the scale of individual slumps, net radiation, summer air temperature, wind and

Table 4

Correlation coefficients (r^2) between 20-yr average headwall retreat rates and various terrain factors extracted from a digital elevation model for 19 active thaw slumps in the study area. Location, terrain characteristics and 20-yr average headwall retreat rates of the 19 thaw slumps are provided in Table 2. Correlations significant at the 10% level are indicated in bold.

Terrain factor	All slumps	Mega-slumps excluded
Surface area	0.14	0.06
Elevation	0.19	0.002
Slope	0.04	0.003
Potential incoming solar radiation	0.11	0.02
Transformed aspect	0.33	0.30
Slope curvature	0.002	0.07
Topographic moisture index	0.09	0.03
Flow accumulation	0.01	0.00

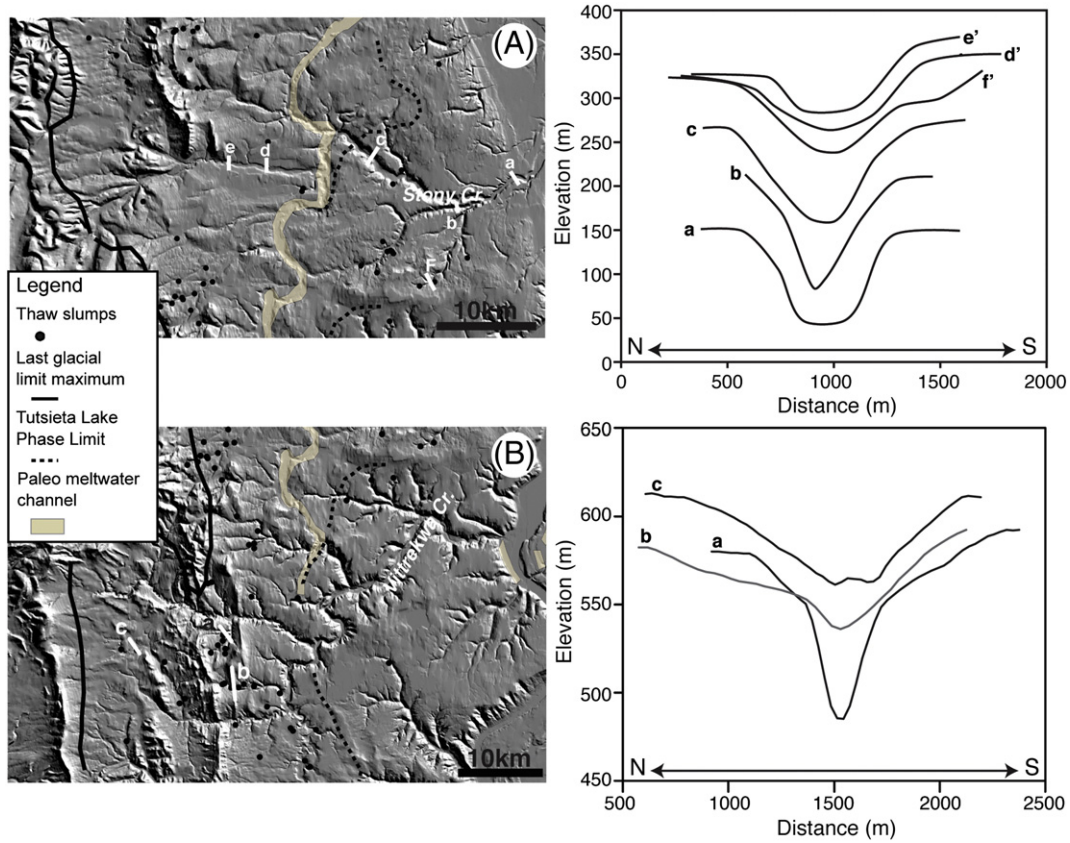


Fig. 9. Topographic cross-sections of nine fluvial valleys in the Stony Creek (A) and Vittrekwa (B) catchments. For most valleys, valley asymmetry is observed with steeper north and east facing slopes.

headwall height are the main factors that drive the ablation of ground ice and headwall retreat rates (Lewkowicz, 1985, 1987; Robinson and Pollard, 1998; Grom and Pollard, 2008; Wang et al., 2009). The findings in these studies were based on climate data derived from a meteorological station located at or in close proximity to the studied thaw slump, which is in contrast to our study where the climate data are derived from the Fort McPherson meteorological station. This suggests that the micro-climate conditions at the scale of individual thaw slump may differ greatly between them, which would explain a lack of relation between the 3-yr running average headwall retreat rates and the regional climate indices for some of the slumps analyzed. Therefore, we focus on discussion on the spatial variation of the 20-yr headwall retreat rates of the 19 thaw slumps in the Richardson Mountains–Peel Plateau region.

For 19 thaw slumps, the 20-year (1990–2010) average headwall retreat rate is $12.4 \pm 7.4 \text{ m yr}^{-1}$. This multi-decadal average headwall retreat rate is similar to those calculated for thaw slumps at other locations in the western Canadian Arctic. For example, slumps situated along the coastline of Hershel Island (YT) yielded an average headwall retreat rate of 9.6 m yr^{-1} for the 1970–2000 period (Lantuit and Pollard, 2008). In central Yukon, 1949–1993 headwall retreat rates for a slump averaged 10 m yr^{-1} (Burn, 2000). In the NWT, thaw slump headwall retreat rates averaged 7 m yr^{-1} in the 1960s on Ellef Ringnes Island, with a maximum of 10 m yr^{-1} (Lamothe and St-Onge, 1961), while on Banks Island, retreat rates averaged 12 m yr^{-1} between 1952 and 1962 (Lewkowicz, 1987).

The 20-yr headwall retreat rates have a statistically significant relation with slope aspect and *PISR*, and near-statistically significant relation with surface area (Table 4). However, if we exclude the two mega-slumps, only slope aspect has a significant relation with 20-yr retreat rates. This suggests two important findings: i) at the regional scale, headwall retreat rates are mainly related to slope aspect, with south- and west-facing slopes exhibiting higher retreat rates; and

ii) mega-slumps are generating feedbacks that allow them to perpetuate their growth. The first finding is consistent with the studies of Lewkowicz (1987) and Grom and Pollard (2008) who suggested that the ablation rate of the exposed ice-rich permafrost is largely dependent on slope orientation. Further, the geometry of the thaw slumps, with steep headwall and slump floor of low angle, allows for snowdrift to accumulate at the base of the headwall. The increased insolation received on south- and west-facing slopes promotes snowmelt and earlier exposure of the slump headwall to summer ablation and a longer thawing season (Fig. 10). As a result, thaw slumps located along south- and west-facing slopes tend to exhibit higher 20-yr average headwall



Fig. 10. Field photograph (late June 2011) showing a portion of the headwall of FM3 thaw slump (field of view is looking north). Residual snowdrift is present on section of headwall exposed to the east.

retreat rates due to higher amount and prolonged insolation that the headwalls receive during the thaw season.

The two mega-slumps have 20-yr average retreat rates that are ranked in the top three highest values calculated in the study area (Table 2), and are among the highest ever determined in the western Canadian Arctic. This suggests that mega-slumps, which have surface area greater than 20 ha, headwall heights up to 40 m and a debris tongue that connects the valley bottom, are generating their own feedbacks that allow them to maintain growth rates well above those of smaller slumps. Based on field measurements (Lewkowicz, 1987; Grom and Pollard, 2008), surface energy fluxes, ground ice and headwall characteristics (height and orientation) control the headwall retreat rate. Mega-slumps are likely situated in areas with high ground ice content that extends to significant depths below the surface. In fact, field observations at two mega-slumps (one of which was included in the headwall retreat rate analysis; FM2 slump) show that the tens of meter high headwall exposes mainly massive ground ice. Further, the taller headwall of mega-slumps allows the ablation of the exposed ice-rich permafrost to start earlier in the thaw season as a significant portion of their headwall is not covered by snowdrift. The ground ice meltwater will transfer sensible heat that will increase the rate of melting of the snowdrift at the base of headwall of mega-slumps. By contrast, small slumps with much shorter headwall heights can remain snow covered well into mid-summer and, as a result, the headwall will only start retreating until the snow covering the headwall has melted. Finally, the high ground ice content combined with the taller headwall heights of mega-slumps allows for higher volume of ground ice meltwater that maintains the slump floor with high moisture level. Time-lapse photographs taken at FM2 slump revealed that the accumulation of materials supplied by thawing ground ice, slumping and toppling of surface material, is being moderately reworked by diurnal ground ice meltwater induced flows (Kokelj et al., 2013). This is compounded during rain-fall events when the already saturated scar zone materials may be removed downslope by significant mass flows (Lacelle et al., 2010). These processes associated with mega-slumps help promote evacuation of materials from the slump floor which maintain a headwall of exposed ice and to experience continued growth. This ensures that periods of stabilization are less likely to punctuate periods of activity, which would result in lower 20-yr average rates of retreat. Overall, it is suggested that the high ground ice content and headwall characteristics of mega-slumps allow these disturbances to generate positive feedbacks that allow them to sustain retreat rates higher than smaller slumps.

6. Conclusions

This study investigated terrain controls on the distribution and growth of thaw slumps in the Richardson Mountains and Peel Plateau region, northwestern Canada, one of the most rapidly warming regions in the Arctic. An inventory of active and stable thaw slumps was developed using the TC trend analysis of a dense Landsat image stack. In the study area, more than 212 thaw slumps have been identified, of which 189 have been active since at least 1985. The Willow River, Stony Creek and Vittrekwa Creek catchments contain more than 60% of all slumps, while the total surface area of these catchments occupies only 25% of the study area. The region also contains some of the largest thaw slumps in the circum-Arctic, with 10 slumps exceeding 20 ha in surface area. These mega-slumps are all active and the sum of their surface area accounts for 28% of all mapped active slumps. The thaw slumps are all situated within the maximum extent of the Laurentide Ice Sheet and 69% of them are constrained between the glacial limit and the Tutsieta Lake Phase limit. Based on relations between frequency distribution of slumps and that of terrain factors in the landscape, the slumps are more likely to occur on the ice-rich hummocky rolling moraines at elevations of 300–350 m and 450–500 m and along east-facing slopes (slope aspects of 15° to 180°) with gradients of 8° to 12°. As such, the distribution of thaw slumps reflects general landscape morphology

associated with east facing regional slope and the ongoing fluvial processes and stream network development that have produced moderately steep hillslopes.

Pixel-level analysis of the TC greenness transformation in the stack of Landsat scenes allowed deriving 3-yr running average and 20-yr average headwall retreat rates of 19 thaw slumps. The 20-yr average headwall retreat rates ranged from 7.2 to 26.7 m yr⁻¹, with the two mega-slumps in the analysis having retreat rates that ranked in the top three highest values calculated in the study area and are among the highest ever determined in the western Canadian Arctic. Statistical analysis revealed that 20-yr headwall retreat rates are largely controlled by slope aspect. These two findings suggest that, at the regional scale, headwall retreat rates are mainly related to slope aspect, with south- and west-facing slopes exhibiting higher retreat rates and that mega-slumps are generating their own feedbacks that allow them to maintain growth rates well above those of smaller slumps.

Acknowledgments

This work was supported by the Natural Sciences and Engineering Research Council of Canada (NSERC) Discovery Grant and Northwest Territories Cumulative Impact Monitoring Program, with logistical support provided by NSERC Northern Supplement, Polar Continental Shelf Program and Northern Scientific Training Program. We would like to thank S. Tetlich, C. Vaneltzi, B. Wilson and J. Wilson for their valuable field assistance. We also thank the two reviewers (J. Vandenberghe and I.S. Evans) and editor T. Oguchi for their constructive comments on the manuscript.

References

- Aylsworth, J.M., Burgess, M.M., Desrochers, D.T., Duk-Rodkin, A., Robertson, T., Traynor, J.A., 2000. Surficial geology, subsurface materials, and thaw sensitivity of sediments. The Physical Environment of the Mackenzie Valley, Northwest Territories: A Base Line for the Assessment of Environmental Change 547 p. 41.
- Beers, T.W., Dress, P.E., Wensel, L.C., 1966. Aspect transformation in site productivity research. *J. For.* 64, 691–692.
- Beirle, B.D., 2002. Late Quaternary glaciation in the Northern Ogilvie Mountains: revised correlations and implications for the stratigraphic record. *Can. J. Earth Sci.* 39, 1709–1717.
- Benn, D.I., Evans, D.J.A., 2010. *Glaciers and Glaciation*. Routledge, New York, USA (802 pp.).
- Beven, K.J., Kirkby, M.J., 1979. A physically based, variable contributing area model of basin hydrology. *Hydrol. Sci. Bull.* 24, 43–69.
- Brooker, A., Fraser, R.H., Olthof, I., Kokelj, S.V., Lacelle, D., 2014. Mapping the activity and evolution of retrogressive thaw slumps by Tasseled Cap trend analysis of a Landsat satellite image stack. *Permafrost. Periglac. Process.* 25, 243–256.
- Burn, C.R., 2000. The thermal regime of a retrogressive thaw slump near Mayo, Yukon Territory. *Can. J. Earth Sci.* 37, 967–981.
- Burn, C.R., Friele, P.A., 1989. Geomorphology, vegetation succession, soil characteristics and permafrost in retrogressive thaw slumps near Mayo, Yukon Territory. *Arctic* 42, 31–40.
- Burn, C.R., Kokelj, S.V., 2009. The permafrost and environment of the Mackenzie Delta area. *Permafrost. Periglac. Process.* 20, 83–105.
- Burn, C.R., Lewkowicz, A.G., 1990. Retrogressive thaw slumps. *Can. Geogr.* 34, 273–276.
- Catto, N.R., 1996. Richardson Mountains, Yukon-Northwest Territories: the northern portal of the postulated 'ice-free' corridor. *Quat. Int.* 32, 3–19.
- Chander, G., Markham, B.L., Helder, D.L., 2009. Summary of current radiometric calibration coefficients for Landsat MSS, TM, ETM+, and EO-1 ALI sensors. *Remote Sens. Environ.* 113, 893–903.
- Cote, M.M., Duchesne, C., Wright, J.F., Ednie, M., 2013. Digital compilation of the surficial sediments of the Mackenzie Valley corridor, Yukon Coastal Plain, and the Tuktoyaktuk Peninsula. Geological Survey of Canada, Open File 7289p. 38. <http://dx.doi.org/10.4095/292494>.
- Couture, R., Riopel, S., 2007. Landslide Inventory Spatial Database for a Study along a Proposed Gas Pipeline Corridor between Inuvik and Tulita, Mackenzie Valley, Northwest Territories. Geological Survey of Canada, Ottawa, Canada (Open File 5740).
- Duk-Rodkin, A., Hughes, O.L., 1992. Map 1745A: Surficial Geology: Fort McPherson - Bell River, Yukon - Northwest Territories. Geological Survey of Canada.
- Dyke, L., 2004. Stability of frozen and thawing slopes in the Mackenzie Valley, Northwest Territories. 57th Canadian Geotechnical Conference/5th Joint CGS/IAH-CNC Conference. Quebec, Canada, pp. 31–38.
- Ecosystem Classification Group, 2010. *Ecological Regions of the Northwest Territories – Cordillera*. Department of Environment and Natural Resources, Government of the Northwest Territories, Yellowknife, NT, Canada (245 pp.).
- Environment Canada, 2012. National climate data and information archive, Fort McPherson, NWT. <http://climate.weatheroffice.gc.ca>.

- Fraser, R.H., Olthof, I., Carrière, D.A., Pouliot, D., 2011. Detecting long-term changes to vegetation in northern Canada using the Landsat satellite image archive. *Environ. Res. Lett.* 6, 045502 (9 pp.).
- Fraser, R., Olthof, I., Carrière, M., Deschamps, A., Pouliot, D., 2012. A method for trend-based change analysis in Arctic tundra using the 25-year Landsat archive. *Polar Rec.* 48, 83–93.
- Fraser, R.H., Olthof, I., Kokelj, S.V., Lantz, T.C., Lacelle, D., Brooker, A., Wolfe, S., Schwarz, S., 2014. Detecting landscape changes in high latitude environments using Landsat trend analysis: 1. Visualization. *Remote Sens.* 6, 11533–11557.
- French, H.M., 1974. Active thermokarst processes, eastern Banks Island, western Canadian Arctic. *Can. J. Earth Sci.* 11, 785–794.
- French, H.M., 2007. *The Periglacial Environment*. 3rd edition. John Wiley and Sons Ltd., Chichester, England (458 pp.).
- Grom, J.D., Pollard, W.H., 2008. A study of high Arctic retrogressive thaw slump dynamics, Eureka Sound Lowlands, Ellesmere Island. In: Kane, D.L., Hinkel, K.M. (Eds.), *Proceedings of the Ninth International Conference on Permafrost*, 29 June–3 July 2008, Fairbanks, Alaska. Fairbanks Alaska. Institute of Northern Engineering, University of Alaska Fairbanks, pp. 545–550.
- Heginbottom, J.A., Radburn, L.K., 1992. *Permafrost and Ground Ice Conditions of North-western Canada (Mackenzie Region)*. National Snow and Ice Data Center, Boulder, CO, USA.
- Hughes, O.L., Hodgson, D.A., Pilon, J., 1972. Surficial geology, Fort Good Hope, Arctic Red River, Fort McPherson, District of Mackenzie, maps and legend; Geological Survey of Canada, Open File 97, scale 1:125,000.
- Kokelj, S.V., Zajdlik, B., Thompson, M.S., 2009. The impacts of thawing permafrost on the chemistry of lakes across the subarctic boreal–tundra transition, Mackenzie Delta region, Canada. *Permafr. Periglac. Process.* 20, 185–199.
- Kokelj, S.V., Lacelle, D., Lantz, T.C., Tunnicliffe, J., Malone, L., Clark, I.D., Chin, K., 2013. Thawing of massive ground ice in mega slumps drives increases in stream sediment and solute flux across a range of watershed scales. *J. Geophys. Res. Earth Surf.* 118, 1–12.
- Lacelle, D., Bjornson, J., Lauriol, B., Clark, I.D., Troutet, Y., 2004. Segregated-intrusive ice of subglacial meltwater origin in retrogressive thaw flow headwalls, Richardson Mountains, NWT, Canada. *Quat. Sci. Rev.* 23, 681–696.
- Lacelle, D., Lauriol, B., Clark, I.D., Cardyn, R., Zdanowicz, C., 2007. Nature and origin of a Pleistocene-age massive ground-ice body exposed in the Chapman Lake moraine complex, central Yukon Territory, Canada. *Quat. Res.* 68, 249–260.
- Lacelle, D., Bjornson, J., Lauriol, B., 2010. Climatic and geomorphic factors affecting contemporary (1950–2004) activity of retrogressive thaw slumps on the Aklavik Plateau, Richardson Mountains, NWT, Canada. *Permafr. Periglac. Process.* 21, 1–15.
- Lacelle, D., Lauriol, B., Zazula, G.D., Ghaleb, B., Utting, N., Clark, I.D., 2013. Timing of advance and basal condition of the Laurentide Ice Sheet during the last glacial maximum in the Richardson Mountains, NWT. *Quat. Res.* 80, 274–283.
- Lamothe, C., St-Onge, D., 1961. A note on a periglacial erosional process in the Isachsen area, N.W.T. *Geogr. Bull.* 16, 104–113.
- Lantuit, H., Pollard, W.H., 2005. Temporal stereophotogrammetric analysis of retrogressive thaw slumps on Herschel Island, Yukon Territory. *Nat. Hazards Earth Syst. Sci.* 5, 413–423.
- Lantuit, H., Pollard, W.H., 2008. Fifty years of coastal erosion and retrogressive thaw slump activity on Herschel Island, southern Beaufort Sea, Yukon Territory, Canada. *Geomorphology* 95, 84–102.
- Lantuit, H., Pollard, W.H., Couture, N., Fritz, M., Schirmer, L., Meyer, H., Hubberten, H.-W., 2012. Modern and late Holocene retrogressive thaw slump activity on the Yukon coastal plain and Herschel Island, Yukon Territory, Canada. *Permafr. Periglac. Process.* 23, 39–51.
- Lantz, T.C., Kokelj, S.V., 2008. Increasing rates of retrogressive thaw slump activity in the Mackenzie Delta region, N.W.T. Canada. *Geophys. Res. Lett.* 35, L06502. <http://dx.doi.org/10.1029/2007GL032433>.
- Lantz, T.C., Kokelj, S.V., Gergel, S.E., Henry, G.H.R., 2009. Relative impacts of disturbance and temperature: persistent changes in microenvironment and vegetation in retrogressive thaw slumps. *Glob. Chang. Biol.* 15, 1664–1675.
- Leibman, M., Gubarkov, A., Khomutov, A., Kizyakov, A., Vanshtein, B., 2008. Coastal processes at the tabular-ground-ice-bearing area, Yugorsky Peninsula, Russia. In: Kane, D.L., Hinkel, K.M. (Eds.), *Ninth International Conference on Permafrost*. University of Alaska Fairbanks, USA, pp. 1037–1042.
- Lewkowicz, A.G., 1985. Use of an ablatometer to measure short-term ablation of exposed ground ice. *Can. J. Earth Sci.* 22, 1767–1773.
- Lewkowicz, A.G., 1987. Headwall retreat of ground-ice slumps, Banks Island, Northwest Territories. *Can. J. Earth Sci.* 24, 1077–1085.
- Malone, L., Lacelle, D., Kokelj, S.V., Clark, I.D., 2013. Impacts of hillslope thaw slumps on the geochemistry of permafrost catchments (Stony Creek watershed, NWT, Canada). *Chem. Geol.* 356, 38–49.
- Moorman, B.J., Michel, F.A., 2000. The burial of ice in the proglacial environment on Bylot Island, Arctic Canada. *Permafr. Periglac. Process.* 11, 161–175.
- Robinson, S.D., Pollard, W.H., 1998. Massive ground ice within Eureka Sound, Ellesmere Island, Canada. In: Lewkowicz, A.G., Allard, M. (Eds.), *Seventh International Permafrost Conference*, St-Foy, QC, Canada, *Nordica* No. 57, pp. 949–954.
- Serreze, M.C., Walsh, J.E., Chapin, F.S., Osterkamp, T.E., Dyurgerov, M., Romanovsky, V., Oechel, W.C., Morison, J., Zhang, T., Barry, R.G., 2000. Observational evidence of recent change in the northern high-latitude environment. *Climate Change* 46, 159–207.
- Smith, I.R., Lesk-Winfield, K., 2012. An updated assessment of ground ice and permafrost geology-related observations based on seismic shothole drillers' log records, Northwest Territories and northern Yukon. Geological Survey of Canada, Open File 7061. <http://dx.doi.org/10.4095/290974> (1 DVD).
- Swanson, D.K., 2012. *Monitoring of Retrogressive Thaw Slumps in the Arctic Network, 2011: Three-Dimensional Modeling of Landform Change*. Natural Resource Report NPS/ARC/NRDS–2012/247. National Park Service, Fort Collins, Colorado, p. 60.
- Thienpont, J.R., Ruhland, K.M., Pisarcic, M.F.J., Kokelj, S.V., Kimpe, L.E., Blais, J.M., Smol, J.P., 2013. Biological responses to permafrost thaw slumping in Canadian Arctic lakes. *Freshw. Biol.* 58, 337–353.
- Wang, B., Paudel, B., Li, H., 2009. Retrogression characteristics of landslides in fine-grained permafrost soils, Mackenzie Valley, Canada. *Landslides* 6, 121–127.
- Zazula, G.D., Mackay, G., Andrews, T.D., Shapiro, B., Letts, B., Brock, F., 2009. A late Pleistocene steppe bison (*bison priscus*) partial carcass from Tsiigehtchic, Northwest Territories, Canada. *Quat. Sci. Rev.* 28, 25–26.
- Zhu, Z., Woodcock, C.E., 2012. Object-based cloud and cloud shadow detection in Landsat imagery. *Remote Sens. Environ.* 118, 83–94.